



Influence of the growth temperature of AlN buffer on the quality and stress of GaN films grown on 6H–SiC substrate by MOVPE

Shuang Qu^a, Shuqiang Li^{a,b}, Yan Peng^a, Xueliang Zhu^b, Xiaobo Hu^a, Chengxin Wang^b, Xiufang Chen^a, Yuqiang Gao^a, Xiangang Xu^{a,b,*}

^a State Key Laboratory of Crystal Materials, Shandong University, Jinan 250100, PR China

^b Shandong Huaguang Optoelectronics Co. Ltd., Jinan 250101, PR China

ARTICLE INFO

Article history:

Received 9 January 2010
Received in revised form 14 April 2010
Accepted 25 April 2010
Available online 4 May 2010

Keywords:

Organometallic vapor phase epitaxy
Nitrides
Semiconducting silicon compounds
High-resolution X-ray diffraction

ABSTRACT

The influence of AlN buffer growth temperature on the quality and stress of 4.5 μm GaN epilayer on 6H–SiC substrate by organometallic vapor phase epitaxy (MOVPE) has been investigated. The crystalline quality and the atomic surface morphology were improved, the density of the pits and the stress of the GaN epilayer were reduced by increasing the growth temperature of the AlN buffer in the range from 950 °C to 1100 °C. By employing the optimized 1100 °C growth temperature of AlN buffer, very high quality of GaN epilayer was achieved. The X-ray full width of half maximums (FWHMs) of (002) and (102) reflection rocking curves of the GaN epilayer have been improved to 159 arcsec and 194 arcsec, respectively, and the surface RMS to only 0.31 nm in the 5 μm × 5 μm atomic force microscopy (AFM) scan. The stress of GaN epilayer was investigated by X-ray diffraction and Raman scattering as well. The degree of the tensile stress in GaN epilayer could be suppressed by increasing the growth temperature of AlN buffer. Finally, a high quality of crack-free 4.5 μm thick GaN epilayer was obtained on 6H–SiC substrate using the optimized 1100 °C AlN growth temperature.

© 2010 Elsevier B.V. All rights reserved.

1. Introduction

In recent years, great interests in research and development of GaN materials increased rapidly [1–4]. Nitrides have been recognized as the most promising materials for laser diodes (LDs), light emitting diodes (LEDs) and high electron mobility transistors (HEMTs) applications [5–7]. Due to the lack of affordable large area GaN substrates, sapphire (Al₂O₃) [8,9], silicon carbide (SiC) [10,11] and other foreign substrates [12–14] are widely used for nitrides epitaxy growth. 6H–SiC is considered as a better substrate than other substrates for its smaller lattice mismatch with GaN, and its higher thermal conductivity [10,11,15]. The coefficients of thermal expansion, lattice constants, and thermal conductivity for GaN, AlN, 6H–SiC and sapphire are listed in Table 1 [15,16].

The crystalline quality and the stress status of GaN film are important for device fabrication and for GaN growth on 6H–SiC, most researchers used AlN [17–19] as buffer layer to improve GaN quality and reduce the tensile stress of the epilayer. The crystalline quality of GaN epilayer determines the property of the device, thus finding a way to improve the quality of GaN is important for all

researchers. There is a substantial tensile stress in GaN epilayer grown on SiC substrate because of the large mismatch of thermal expansion coefficients between GaN and SiC [20]. Very high density of cracks would be generated by the tensile stress in GaN epilayer. Therefore, reducing the tensile stress is important. Many efforts have been made in order to decrease the tensile stress of GaN grown on SiC. Using AlN/GaN superlattices buffer to reduce the crack had been proposed by Yamamoto et al. [21]; the similar reports were also raised by Kurimoto et al. [22].

The AlN buffer growth condition has great influence on the quality and the stress of GaN epilayer. The growth processes of AlN buffer were studied by Moran et al., they found that threading dislocations were formed at the coalescence boundaries [23]. Chen et al. found that alternating between two-dimensional (2D) and three-dimensional (3D) growth modes could induce a better quality of AlN epilayer [24]. The influence of AlN thickness on GaN quality was investigated by Green et al., they showed that increasing the thickness of the AlN buffer smoothed the AlN but increased the edge dislocation density [25]. Moe et al. studied the influence of substrate nitridation, TMAI flow and V/III ratio on the quality of AlN buffer, in their work long nitridation time, a high TMAI flow and high V/III ratio improved the quality of AlN [26]. Koleske et al. showed the AlN buffer layer growth temperature influences the electrical properties of GaN epilayer grown on SiC [27]. Wong et al. investigated the effect of AlN buffer on the electrical properties

* Corresponding author at: State Key Laboratory of Crystal Materials, Shandong University, Jinan 250100, PR China. Tel.: +86 531 88366329.

E-mail address: xxu@sdu.edu.cn (X. Xu).

Table 1
The coefficients of thermal expansion, lattice constants, and thermal conductivity for GaN, AlN, 6H-SiC and sapphire.

		GaN	AlN	6H-SiC	Sapphire
Coefficients of thermal expansion ($\times 10^{-6} \text{ K}^{-1}$)	<i>a</i>	5.6	4.2	4.2	7.5
	<i>c</i>	3.2	5.3	4.7	8.5
Lattice constants (Å)	<i>a</i>	3.188	3.111	3.081	4.758
	<i>c</i>	5.185	4.979	15.092	12.991
Thermal conductivity (W/cm K)		2.1	2.9	4.2	0.3

of N-face GaN and found that AlN grown in the N-rich regime was essential for realizing highly resistive GaN buffers [28].

In earlier literature, AlN buffer thickness, V/III ratio and the initial 6H-SiC crystalline quality were the most important parameters to control the quality and stress of GaN epilayer [25,26,29]. To the best of author's knowledge, there are few reports [25,30] about the influence of the growth temperature of AlN buffer on the crystalline quality and the stress of GaN epilayer.

In this letter, the influence of the growth temperature of AlN buffer on the structural quality and the stress of GaN epilayer grown on (0001) 6H-SiC substrate by MOVPE were investigated in detail using the X-ray diffraction, atomic force microscopy (AFM) and Raman scattering measurements.

2. Materials and experimental procedures

The samples of GaN/AlN/SiC heterostructures were grown by metal organic vapor phase epitaxy (MOVPE) system on (0001) 6H-SiC from Shandong University. Trimethylaluminum (TMAI), trimethylgallium (TMGa) and ammonia (NH₃) were used as precursors, and SiH₄ as the n-type dopant source. The growth pressure was 500 Torr for GaN growth and 100 Torr for AlN to reduce parasitic chemical reactions. The GaN growth temperature was kept at 1070 °C. The thickness of the AlN buffer layer was designed to be 10 nm. After the AlN buffer, a 1.5 μm thick undoped GaN layer was grown on it, followed by a 3 μm thick Si doped GaN layer. The total thickness of GaN epilayer was 4.5 μm.

Three different growth temperatures, 950 °C (Sample A), 1050 °C (Sample B) and 1100 °C (Sample C), have been tested for the AlN buffer layer while other growth conditions were kept the same to obtain GaN/AlN/SiC heterostructure.

All samples were evaluated by high-resolution X-ray diffraction (HR-XRD). The lattice parameters were determined by (002), (004) and (101), (202) multi-diffraction omega-2theta scan. Raman spectra of the samples were obtained by the LabRAM HR system of Horiba Jobin Yvon at room temperature using the 532 nm solid laser as the exciting source. The E2 (high) phonon peak shift with the depth of GaN was recorded to illustrate the stress track in GaN epilayer. The surface morphology was examined by AFM system.

3. Results and discussion

3.1. Influence of AlN growth temperature on dislocation density and surface morphology of GaN films

Symmetric (002) reflection and asymmetric (102) reflection rocking curves for the three samples are shown in Fig. 1. The FWHMs of (002) and (102) reflection are reduced substantially to 159 arcsec and 194 arcsec from 282 arcsec and 314 arcsec, respectively when increasing the AlN buffer growth temperature from 950 °C to 1100 °C. The peak intensities are also enhanced significantly in the same time.

Assuming the X-ray rocking curve to be a Gaussian distribution in shape, the omega-scan FWHM of (102) reflection can be written as Eq. (1) [31]:

$$\beta_{(102)}^2 = \beta_{\text{screw}}^2 + \beta_{\text{edge}}^2 \quad (1)$$

where β_{screw} and β_{edge} are the contributions of screw and edge dislocations to the omega-scan FWHM of (102) reflection. The dislocation density can be calculated from Eqs. (2) and (3):

$$\rho = \frac{\beta^2}{4.35 \times b_{\text{screw}}^2} \quad (2)$$

For screw dislocation:

$$\rho = \frac{\beta_{(002)}^2}{4.35 \times b_{\text{screw}}^2} = \frac{\beta_{\text{screw}}^2}{4.35 \times b_c^2} \quad (3)$$

where b_c is the component of b_{screw} contributing to the FWHM of (102) reflection, and $b_c = b_{\text{screw}} \times \cos 43.19^\circ$. And in the same way, the edge dislocation density can also be calculated.

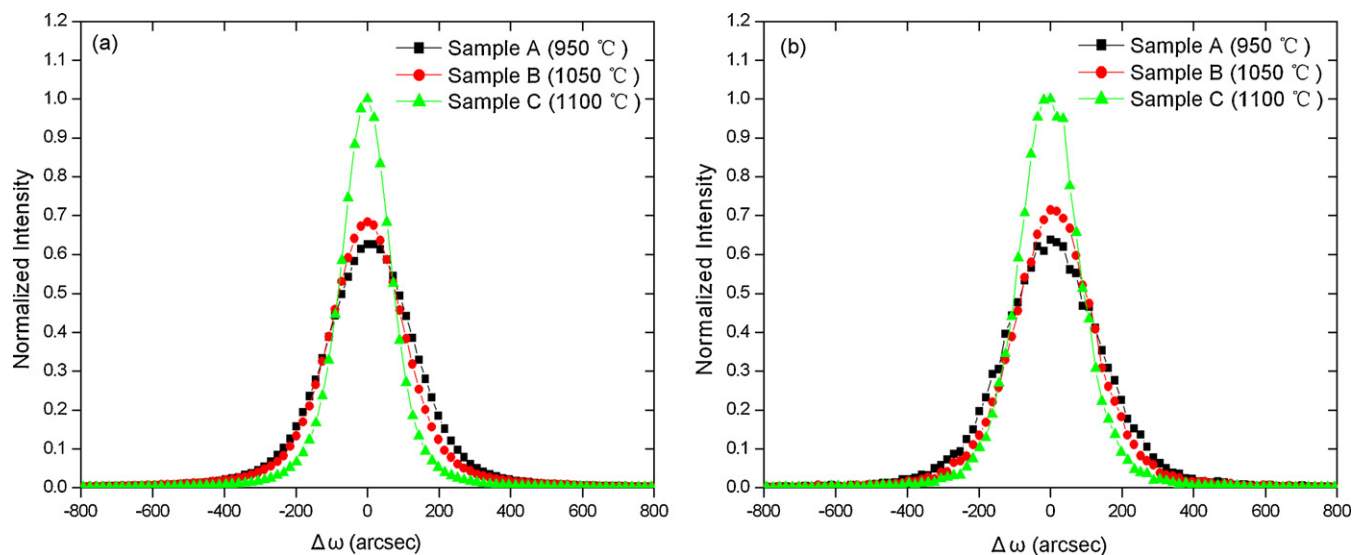


Fig. 1. X-ray rocking curve of the three samples: (a) (002) reflection and (b) (102) reflection.

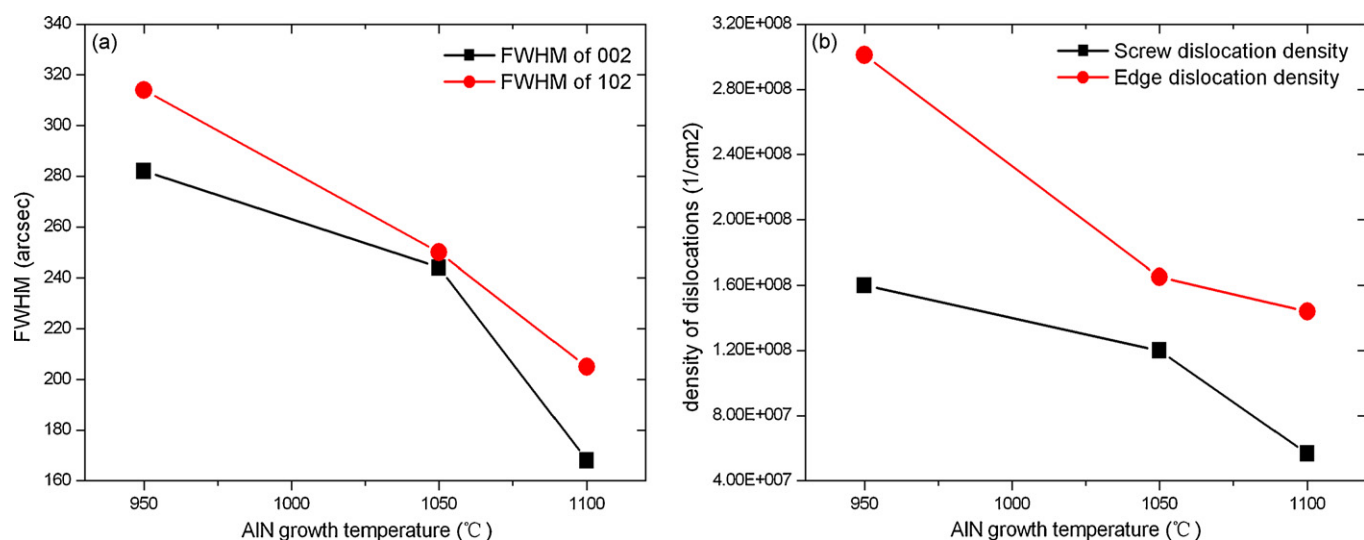


Fig. 2. Relationship between AlN growth temperature and (a) X-ray FWHM; (b) dislocation density. The red and black lines are FWHMs of (102) reflection (density of edge dislocations) and (002) reflection (density of screw dislocations), respectively. (For interpretation of the references to color in this figure caption, the reader is referred to the web version of the article.)

Fig. 2 shows the X-ray omega-scan FWHM and dislocation density of GaN with different AlN buffer growth temperatures. The densities of both screw and edge dislocations are reduced significantly by up to three times with increasing the AlN buffer growth temperature from 950 °C to 1100 °C.

Al active species have a very slow migration on the growth surface, so the AlN buffer grown at low growth temperature, such as 950 °C, may not be a coherent film, resulting in a bad crystalline quality of the subsequent GaN epilayer. High growth temperature can accelerate the Al species' migration on the surface to form an AlN epilayer with better quality [25], therefore, a better quality of GaN epilayer is produced and the dislocation density in the subsequent thick GaN epilayer can be reduced significantly by up to three times.

Fig. 3 shows the AFM images of samples A, B, and C, the roughness roots mean-square (RMS) values of the three samples are 0.395 nm, 0.406 nm, and 0.310 nm, respectively.

For samples A and B whose AlN buffers growth temperatures were 950 °C and 1050 °C, the RMS of GaN films were nearly the same, both was about 0.40 nm. When AlN buffer temperature increased to 1100 °C, the RMS reduced to 0.31 nm substantially. It could be explained as the following: when raising AlN growth temperature, the step-flow of AlN growth was promoted and a smoother AlN surface morphology was obtained. Therefore, the steps of GaN grown afterwards would get flatter, and the surface

terrace of GaN film became obviously wider, resulting in a better quality GaN film with lower density of disordered atomic steps and pits.

Disordered steps and pits are the most widely observed defects on GaN film surface. The disordered atomic steps were reported to originate from screw- or mixed-type dislocations and the pits were caused by edge-type dislocations [32], therefore, the screw- or mixed-type dislocations disturb the atomic steps, whereas edge-type dislocations do not [30]. In our AFM images, the density of pits and disordered atomic steps of the three samples were decreased with increasing of AlN buffer growth temperature. It means the density of dislocations is reduced dramatically, consistent with the result of the X-ray FWHM above.

3.2. Influence of AlN growth temperature on the stress of GaN films

Due to the large mismatch of thermal expansion coefficient between GaN and SiC, the GaN epilayer suffers a significant tensile stress which may cause the film to crack in the worse case, especially when the film is thick. The lattice constant a of AlN is smaller than GaN, which means a compressive stress will be brought to GaN grown on AlN film. Therefore, a high quality AlN buffer layer should be grown before GaN growth is started so that there is a compressive stress in the GaN caused by the lattice mismatch

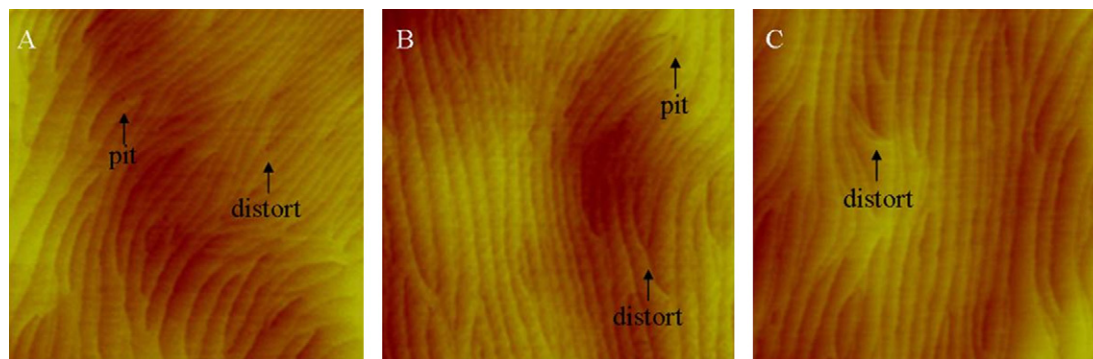


Fig. 3. Surface morphology of samples A, B, and C, whose AlN buffer growth temperatures were 950 °C, 1050 °C, and 1100 °C, respectively. The AFM images were taken over an area of $5 \mu\text{m} \times 5 \mu\text{m}$.

Table 2
The calculated lattice constants of the three samples.

	Sample A (950 °C)	Sample B (1050 °C)	Sample C (1100 °C)	Generally acknowledged value
<i>c</i>	5.186 nm	5.185 nm	5.185 nm	5.185 nm
<i>a</i>	3.192 nm	3.190 nm	3.188 nm	3.188 nm
ε	0.12%	0.06%	0%	–

[33]. The compressive stress would neutralize the tensile stress generated in the cooling down process to obtain a thick crack-free GaN film.

Samples A, B, and C in this work were obtained at different AlN buffer growth temperatures, and different compressive stress exists between AlN and GaN layers in the three samples. The crack density reduced gradually when the AlN growth temperature was raised. It implies that the tensile stress in GaN film decreases with the increase of AlN buffer growth temperature. The stress in the epilayer can be described through the difference between the generally acknowledged lattice constants and the measured lattice constants. The HR-XRD is an effective method to measure the lattice constant of materials. Based on the precision determination of the angular position θ of a reflection hkl , the Bragg law $2d\sin\theta = \lambda$ and the interplanar spacing d , the lattice constants can be determined accurately [34].

The angular position of hkl reflection peak could be obtained from the omega-2theta scan. The GaN (002), (004) and (101), (202) multi-diffraction peak position was used to calculate the lattice constants c and a by the following equations:

$$d_{hkl} = \frac{\lambda}{2 \sin(\theta_{hkl} + \Delta\theta)} = \frac{2\lambda}{2 \sin(\theta_{2h2k2l} + \Delta\theta)} \quad (4)$$

$$d_{hkl} = \frac{1}{\sqrt{\frac{4}{3} \left(\frac{h^2 + hk + k^2}{a} \right)^2 + \left(\frac{l}{c} \right)^2}} \quad (5)$$

where (hkl) is the diffraction plane, θ_{hkl} is the measured angular position of (hkl) reflection, $\Delta\theta$ is the zero error of the instrument, λ is the wavelength of the X-ray (0.154 nm for Cu $K_{\alpha 1}$ radiation).

The calculated lattice constants and tensile strains are listed in Table 2 [15].

As seen in Table 2, the c constants were nearly the same in all the three samples, but the lattice constant a decreased with the increase of the AlN buffer growth temperature. The Poisson's ratio γ in GaN is about 0.37 [35], which mean a constant has two times larger changes than c constants when the GaN material is under stress. The in-plane strains in Table 2 were calculated by formula (6):

$$\varepsilon = \frac{a - a_0}{a_0} \quad (6)$$

From the strain results, the samples with low AlN buffer growth temperature (950 °C and 1050 °C) suffered tensile stress which can be suppressed by increasing the AlN buffer growth temperature to 1100 °C. When the AlN buffer was grown at 1100 °C, the strain of GaN film was zero. In other words, crack-free GaN film was obtained by growing AlN buffer at 1100 °C.

The AlN buffer on 6H-SiC was under compressive stress because of the 2.6% in-plane lattice mismatch. For the similar reason, the lattice mismatch of AlN and GaN also provides GaN a compressive stress. When the samples cooled down from GaN growth temperature, the amount of tensile strain induced by postgrowth cooling was about $\Delta T \times \Delta\alpha = 0.14\%$ when the GaN growth temperature was 1000 °C in this study (ΔT is the difference between room temperature and GaN grown temperature; $\Delta\alpha$ is the mismatch of thermal expansion coefficients between AlN and GaN) [20]. So, the compressive strains induced by lattice mismatch before cooling down

of samples A, B and C were -0.02% , -0.08% and -0.14% , respectively. That means the AlN buffer layer grown at 1100 °C gives GaN epilayer greater compressive strain. It can be explained as follows: if AlN film was grown at a lower temperature, the atom diffusion length would be decreased, leading to a three-dimension growth mode, the coalescence of the nuclear island may not occur [24,36]. Therefore, the compressive stress in GaN film generated by a lower growth temperature AlN buffer is not large enough to compensate the tensile stress which is brought by the cooling down process. In addition, the thermal expansion coefficients of AlN are larger than that of SiC, if AlN was grown in a higher temperature, the lattice constant a of AlN contracts more upon cooling than that of 6H-SiC, so the mismatch of lattice constant between 6H-SiC and AlN would be larger. As a result, the AlN would suffer a larger compressive strain at the initial growth state, so did the GaN layer. Therefore, a high AlN growth temperature will result in the growth of a nearly stress-free GaN film.

The stress could also be determined by the peak shifts in the Raman spectroscopy measurement.

The Raman scattering spectra of sample C are shown in Fig. 4. The E2 (high) phonon is known to shift by in-plane stress only [37]. It was utilized to characterize the stress state in GaN epilayer. From the most results, 568 cm^{-1} is considered to be a precise value for E2 (high) phonon frequency of a stress-free GaN [37]. If the E2 (high) phonon frequency moves to low frequency, it means the GaN film suffers tensile stress. In order to understand the variation of the stress state of the GaN film with the depth, a Z scan from the surface of GaN film towards the substrate was performed.

Fig. 5 shows the results of the Raman shift of E2 (high) phonon of three samples. The blue, red, and yellow lines stand for samples A, B, and C whose AlN growth temperature was 950 °C, 1050 °C and 1100 °C, respectively. The results of $Z=0$ corresponded to the top free surface of GaN film. The depth of GaN film taken in Raman spectra is $4.5 \mu\text{m}$.

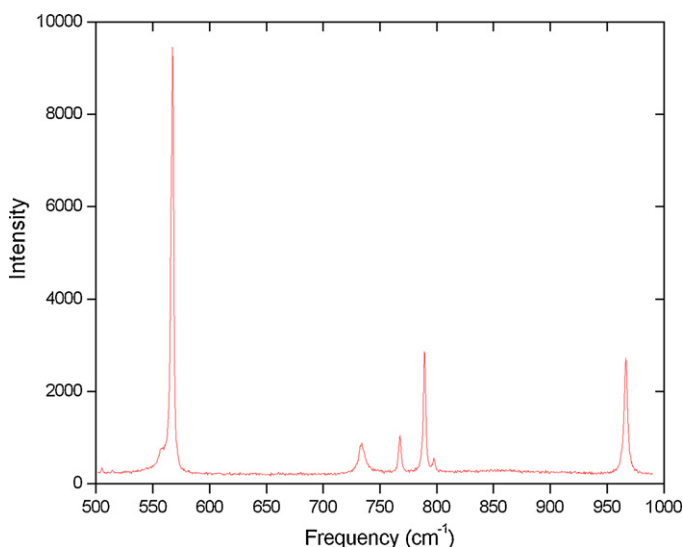


Fig. 4. Raman scattering spectra of sample C.

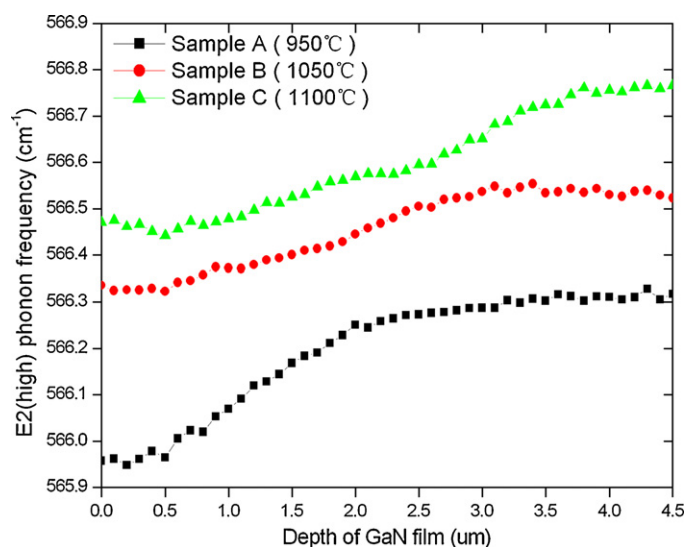


Fig. 5. Raman scattering spectra line of E2 (high) phonon scan along the direction perpendicular to the sample surface. $Z=0$ corresponds to the free surface of the sample.

The E2 (high) phonon frequency of all samples is below 568 cm^{-1} , and the frequency blue-shift occurred with the increase of Z value. It means the tensile strain is the largest at the top free surface of GaN, and it decreases with the increase of the depth of the film.

From the frequencies of E2 (high) phonons of three samples, the frequency blue-shift occurred when the AlN buffer growth temperature was raised. It means the tensile stress was suppressed at a high AlN buffer growth temperature. This result is in a good agreement with the lattice constant measurements from X-ray diffraction.

The stress shift in Fig. 5 can be calculated according to the formula (7) [38]:

$$\sigma = \frac{\Delta\omega}{6.2} \quad (7)$$

The stress gradient of samples A, B, and C from the interface of AlN/GaN to the top surface of GaN was $0.014\text{ GPa}/\mu\text{m}$, $0.009\text{ GPa}/\mu\text{m}$, and $0.009\text{ GPa}/\mu\text{m}$, respectively. Sample A has the biggest stress gradient. Threading dislocations could induce tensile strain and the tensile strain increases with increasing dislocation density [39]. From the X-ray rocking curve results, sample A with 950°C AlN buffer growth temperature has the largest dislocation density. So, the biggest stress gradient of sample A is caused by its largest dislocation density. Larger dislocation density could induce more tensile strain. Therefore, lower dislocation density is another reason for the acquirement of crack-free GaN with 1100°C AlN growth temperature.

4. Conclusions

The influence of AlN buffer growth temperature on the quality and stress of $4.5\text{ }\mu\text{m}$ GaN epilayer on 6H-SiC substrate has been investigated. The AlN buffer growth temperature, which was as important as thickness and V/III ratio, was verified as a key parameter to control the quality and the stress of GaN film grown afterwards. The crystalline quality, the density of the pits, the atomic surface morphology and the stress of the GaN epilayer can be influenced by the growth temperature of the AlN buffer. With increasing the AlN buffer growth temperature from 950°C to 1100°C , X-ray FWHMs of (002) and (102) reflection rock-

ing curve of the GaN epilayer have been significantly improved to 159 arcsec and 194 arcsec , respectively, and the surface RMS to only 0.31 nm in the $5\text{ }\mu\text{m} \times 5\text{ }\mu\text{m}$ atomic force microscopy (AFM) scan. The tensile stress was decreased while raising the AlN buffer growth temperature, which was confirmed by X-ray and Raman scattering. The suppression of the tensile stress was explained that AlN buffer layer with higher growth temperature imposed larger compressive strain on the GaN at the growth temperature which counteracted the effects caused by cooling down process to the room temperature. At last, a high quality crack-free $4.5\text{ }\mu\text{m}$ thick GaN epilayer has been successfully obtained on 6H-SiC substrate by using the optimized 1100°C AlN growth temperature.

Acknowledgements

This work was supported by the National Natural Science Foundation of China under grant no. 50472068 and National Basic Research Program of China under grant no. 2009CB930503.

References

- [1] S. Nakamura, MRS Bull. 34 (2009) 101–107.
- [2] I. Akasaki, J. Cryst. Growth 300 (2007) 2–10.
- [3] D. Peng, Y. Feng, H. Niu, J. Alloys Compd. 476 (2009) 629–634.
- [4] Y.K. Fu, C.H. Kuo, C.J. Tun, L.C. Chang, Solid-State Electron. 54 (2010) 590–594.
- [5] D.G. Zhao, D.S. Jiang, J.J. Zhu, H. Wang, Z.S. Liu, S.M. Zhang, Y.T. Wang, Q.J. Jia, H. Yang, J. Alloys Compd. 489 (2010) 461–464.
- [6] Z. Chen, Y. Pei, S. Newman, R. Chu, D. Brown, R. Chung, S. Keller, S.P. Denbaars, S. Nakamura, U.K. Mishra, Appl. Phys. Lett. 94 (2009) 112108–112110.
- [7] C.F. Shih, K.T. Hung, C.Y. Hsiao, S.C. Shu, W.M. Li, J. Alloys Compd. 480 (2010) 541–546.
- [8] D.-S. Wu, H.-W. Wu, S.-T. Chen, T.-Y. Tsai, X. Zheng, R.-H. Horng, J. Cryst. Growth 311 (2009) 3063–3066.
- [9] T. Bohnen, A.E.F. de Jong, W.J.P. vanEnckevort, J.L. Weyher, G.W.G van Dremel, H. Ashraf, P.R. Hageman, E. Vlieg, J. Cryst. Growth 311 (2009) 4685–4691.
- [10] J. Edmonda, A. Abare, M. Bergman, J. Bharathan, K.L. Bunker, D. Emerson, K. Haberern, J. Ibbetson, M. Leung, P. Russel, D. Slater, J. Cryst. Growth 272 (2004) 242–250.
- [11] V. Harle, B. Hahm, H.J. Lugauer, S. Bader, G. Bruderl, J. Baur, D. Eisert, U. Strauss, U. Zehnder, A. Lell, N. Hiller, Phys. Stat. Sol. A 180 (2000) 5–13.
- [12] J. Zou, W. Xiang, J. Alloys Compd. 484 (2009) 622–625.
- [13] C. Xue, Y. Wang, H. Zhuang, Z. Wang, Y. Huang, D. Zhang, Y. Cao, J. Alloys Compd. 484 (2009) 33–35.
- [14] M. Zielinski, M. Portail, S. Roy, T. Chassagne, C. Moisson, S. Kret, Y. Cordier, Mater. Sci. Eng. B 165 (2009) 9–14.
- [15] L. Liu, J.H. Edgar, Mater. Sci. Eng. B 37 (2002) 61–127.
- [16] F.A. Ponce, B.S. Krusor, J.S. Major Jr., W.E. Plano, D.F. Welch, Appl. Phys. Lett. 67 (1995) 410–412.
- [17] T.W. Weeks, M.D. Bremser, K.S. Ailey, E. Carlson, W.G. Perry, R.F. Davis, Appl. Phys. Lett. 67 (1995) 401–403.
- [18] Z.J. Reitmeier, S. Einfeldt, R.F. Davis, X. Zhang, X. Fang, S. Mahajan, Acta Mater. 58 (2010) 2165–2175.
- [19] Z.J. Reitmeier, S. Einfeldt, R.F. Davis, X. Zhang, X. Fang, S. Mahajan, Acta Mater. 57 (2009) 4001–4008.
- [20] P. Waltereit, O. Brandt, A. Trampert, M. Ramsteiner, M. Reiche, M. Qi, K.H. Ploog, Appl. Phys. Lett. 74 (1999) 3660–3662.
- [21] J. Yamamoto, M. Kurimoto, M. Shibata, T. Honda, H. Kawanishi, J. Cryst. Growth 180/190 (1998) 193–196.
- [22] M. Kurimoto, T. Nakada, Y. Ishihara, M. Shibata, T. Takano, J. Yamamoto, T. Honda, H. Kawanishi, Phys. Stat. Sol. A 176 (1999) 665–669.
- [23] B. Moran, F. Wu, A.E. Romanov, U.K. Mishra, S.P. Denbaars, J.S. Speck, J. Cryst. Growth 273 (2004) 38–47.
- [24] Z. Chen, S. Newman, D. Brown, R. Chung, S. Keller, U.K. Mishra, S.P. Denbaars, S. Nakamura, Appl. Phys. Lett. 93 (2008) 191906–1–191906–3.
- [25] D.S. Green, S.R. Gibb, B. Hosse, R. Veturly, D.E. Grider, J.A. Smart, J. Cryst. Growth 272 (2004) 285–292.
- [26] C.G. Moe, Y. Wu, S. Keller, J.S. Speck, S.P. DenBaars, D. Emerson, Phys. Stat. Sol. A 203 (2006) 1708–1711.
- [27] D.D. Koleske, R.L. Henry, M.E. Twigg, J.C. Culbertson, S.C. Binari, A.E. Wickenden, M. Fatemi, Appl. Phys. Lett. 80 (2002) 4372–4374.
- [28] M.H. Wong, Y. Pei, J.S. Speck, U.K. Mishra, Appl. Phys. Lett. 94 (2009) 182103–182105.
- [29] S. Yamada, J.I. Kato, S. Tanaka, I. Suemune, A. Avramescu, Y. Aoyagi, N. Teraguchi, A. Suzuki, Appl. Phys. Lett. 78 (2001) 3612–3614.
- [30] M. Imura, H. Sugimura, N. Okada, M. Iwaya, S. Kamiyama, H. Amano, I. Akasaki, A. Bandoh, J. Cryst. Growth 310 (2008) 2308–2313.

- [31] J.C. Zhang, D.G. Zhao, J.F. Wang, Y.T. Wang, J. Chen, J.P. Liu, H. Yang, *J. Cryst. Growth* 268 (2004) 24–29.
- [32] T. Hino, S. Tomiya, T. Miyajima, K. Yanashima, S. Hashimoto, M. Ikeda, *Appl. Phys. Lett.* 76 (2000) 3421–3423.
- [33] J.D. Acord, S. Raghavan, D.W. Snyder, J.M. Redwing, *J. Cryst. Growth* 272 (2004) 65–71.
- [34] M.F. Wu, S.Q. Zhou, A. Vantomme, Y. Huang, H. Wang, H. Yang, *J. Vac. Sci. Technol. A* 24 (2006) 275–279.
- [35] J. Elsner, R. Jones, P.K. Sitch, V.D. Porezag, M. Elsner, Th. Frauenheim, M.I. Heggie, S. Oberg, P.R. Briddon, *Phys. Rev. Lett.* 79 (1997) 3672–3675.
- [36] Z. Chen, R.S.Q. Fareed, M. Gaevski, V. Adivarahan, J.W. Yang, J. Mei, F.A. Ponce, M.A. Khan, *Appl. Phys. Lett.* 89 (2006) 081905–081907.
- [37] D. Wang, S. Jia, K.J. Chen, K.M. Lau, Y. Dikme, P. van Gemmer, Y.C. Lin, H. Kalisch, R.H. Jansen, M. Heuken, *J. Appl. Phys.* 97 (2005) 056103.
- [38] T. Kozawa, T. Kachi, H. Kano, H. Nagase, N. Koide, K. Manabe, *J. Appl. Phys.* 77 (1995) 4389–4392.
- [39] Y. Taniyasu, M. Kasu, T. Makimoto, *J. Cryst. Growth* 298 (2007) 310–315.